Separating Reflections in Human Iris Images for Illumination Estimation

Huiqiong Wang*
Zhejiang University

Stephen Lin
Microsoft Research Asia

Xiaopei Liu*
Huazhong Univ. of Sci. and Tech.

Sing Bing Kang
Microsoft Research

Abstract

A method is presented for separating corneal reflections in an image of human irises to estimate illumination from the surrounding scene. Previous techniques for reflection separation have demonstrated success in only limited cases, such as for uniform colored lighting and simple object textures, so they are not applicable to irises which exhibit intricate textures and complicated reflections of the environment. To make this problem feasible, we present a method that capitalizes on physical characteristics of human irises to obtain an illumination estimate that encompasses the prominent light contributors in the scene. Results of this algorithm are presented for eyes of different colors, including light colored eyes for which reflection separation is necessary to determine a valid illumination estimate.

1 Introduction

Changes in illumination can induce significant variations in the appearance of an object. Since these differences in appearance complicate the identification of objects in computer vision, much attention has focused on estimating the lighting conditions in a scene so that its effects can be accounted for. Recovering scene illumination from a given image, however, has proven to be a challenging problem that has only been addressed in rather limited situations.

Because of the direct effects of illumination on shading, shadows and specular reflections, previous works have examined these appearance features to infer lighting information. Shading-based methods for single-image input generally solve for light intensities from a discrete set of directions by analyzing brightness values according to a given reflectance model [24, 7]. Techniques that utilize shadows attached to an object seek to identify pixels that lie along the shadow boundaries, since they indicate the existence of light from a direction perpendicular to its surface normal [23, 22]. For cast shadows that fall onto the object's surroundings, brightness values within the shadows have been used in solving a system of equations for light source intensities at sampled directions [16, 18, 17].

While these shading and shadow based methods have produced accurate estimation results, certain assumptions reduce their applicability. Object textures need to be known or uniform, since texture color variations modulate brightness values. The geometry of the object also must be known to analyze image intensities or shadow formations.

Methods based on specular reflections are also dependent on known object attributes, and similar to shading and shadow based techniques, they generally handle this problem by introducing a reference object of known shape and reflectance into the scene. Most commonly, the object used is a mirrored sphere [2], on which a detailed image of the illumination environment can be seen.

While mirrored spheres do not often appear by chance in general scenes, a similar object that is frequently seen in images is human eyes. Eyes exhibit a significant amount of specular reflection, and have a geometry that is fairly constant from person to person [5]. From eyes, a detailed estimate of frontal illumination could potentially be derived, and could provide much utility in the analysis of faces, which substantially change in appearance with respect to lighting conditions [12].

The use of eyes for imaging the surrounding environment was proposed by Nishino and Nayar [14, 13]. From eye images, they demonstrated various uses of the acquired reflections of the environment, such as computing retinal images, binocular stereo and face relighting. In these methods, the color and texture of the eyes are not separated from the reflected environment.

*This work was done while Huiqiong Wang and Xiaopei Liu were interns at Microsoft Research Asia.

Although the subtle texture of dark colored eyes may not significantly distort the appearance of the environment, irises of light color such as blue or green may substantially obscure reflections of the scene. To determine a more accurate estimate of illumination from the environment, iris colors and textures should be separated from the specularly reflected light, and it is this separation in iris images that is the focus of our work.

There exists much previous work on separating specular reflections from images, but they address relatively restrictive scenarios. Among methods that use single-image input, some identify clusters of specular colors in an RGB histogram and project their points onto clusters of diffuse colors to remove specular reflections [9]. Because of problems that arise from histogram clutter, this approach is generally effective only for textureless surfaces and a constant illuminant color. Recent methods have been proposed for handling surfaces with simple texture [21, 20], but they require specular reflections to be formed from a single illumination color. Because of these limitations, these previous techniques are not suitable for extracting multi-colored reflections of an illumination environment from a highly textured iris. A general separation method based on minimizing the amount of edges and corners in two decomposed images has been presented [11], but textures in irises have complex edge characteristics and smooth color variations that are problematic for such an approach.

To separate reflections on irises, we propose a method that takes advantage of physical iris characteristics to make the problem manageable. Among these iris features are chromaticity properties, radial autocorrelation of iris textures, and the occurrence of irises in pairs, which provides two observations of the illumination environment. To match corresponding observations of the environment in a pair of irises, we present a method for reducing the effects of iris color and texture on the matching process. With these iris constraints, prominent components in the illumination environment can be separated in the iris image to give an illumination estimate for the surrounding scene. In this work, we focus on the separation process, and assume that the iris and pupil areas in an image have been located by an automatic method such as in [6, 14].

2 Iris Features

Although different irises are distinct enough for biometric identification, their physical structure gives rise to certain common color and texture characteristics. In this section, we describe the human eye and the features of irises that are utilized in our technique.

As light enters the eye, it first passes through a transparent protective layer called the cornea, from which much light is specularly reflected. It is this reflection that we aim to recover in estimating the illumination environment. The shape of the cornea is fairly constant for humans, and the section of the cornea that covers the iris can be closely approximated by a partial sphere of radius 7.8 mm that has a maximum circular cross-section of diameter 11.6 mm [5].

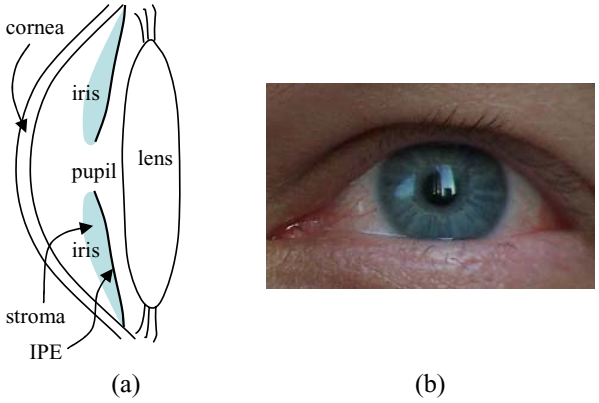

Figure 1. Iris features. (a) Structure of eye; (b) Radial iris texture.

The light then travels through an opening called the pupil, shown in Fig. 1(a), before passing through the lens and onto the retina, which senses the light. The amount of light that passes through the pupil is regulated by the iris, a thin diaphragm composed mostly of connective tissue and smooth muscle fibers. One feature of irises, and eyes, is that they generally appear in pairs. Our illumination estimation method takes advantage of this characteristic, as well as properties of iris color and texture.

2.1 Color

Structurally, the iris contains two different layers. As illustrated in Fig. 1(a), the thin innermost layer is called the iris pigment epithelium (IPE) and consists of a compact array of opaque cells. The outermost layer is referred to as the iris stroma, which contains more loosely arranged cells, including melanocytes that synthesize the pigment melanin.

From the iris structure, there are three principal elements that contribute to its color [8]. One is the pigment in the IPE, which is black in irises of all colors. Another is the melanin content in the iris stroma, which is the primary cause of color variations among different irises [15]. Brown irises have a large amount of melanin, which absorbs much of the incoming light especially at short wavelengths. For blue irises which have low melanin content in the stroma, long-

wavelength light penetrates the stroma and is absorbed in the IPE, while short-wavelength light undergoes Rayleigh scattering and reflection. Green and hazel irises are products of moderate amounts of melanin.

The spectrum of iris colors basically results from varying amounts of stroma melanin. From this property, it has been empirically shown that the distribution of iris chromaticities lies approximately along a line [3]. In our work, we predetermine a gamut line of iris chromaticities by least squares line fitting to diffuse chromaticity values of different color irises measured under controlled lighting conditions. This data is then used in determining eye color and in identifying parts of an iris that have little obscuration by specular reflections.

The third structural component that influences color is the cellular density of the iris stroma. In an area of low density, little light is reflected by the semi-transparent stroma, so it shows the black color of the IPE. Supposing the melanin content to be evenly dispersed among stroma cells, variations of cellular density throughout an iris exhibit the same chromaticity. We use this information to partially differentiate between iris texture and illumination colors.

2.2 Texture

The pattern of fibrovascular tissue in an iris accounts for the stroma cellular density and accordingly the texture seen in irises. As shown in Fig. 1(b), these bands of connective tissue generally extend in the radial direction, and are called radial furrows. Because of this tissue structure, irises exhibit significant radial autocorrelation of colors. In our technique, we utilize this property as a texture constraint in separating reflected illumination from an iris image.

3 Separation Algorithm

Using the characteristics of irises, we formulate an algorithm for separating the specular reflections on the cornea from the iris texture. Although there may exist slight specular reflections from the iris itself, they are generally of negligible magnitude, so we consider the iris texture to be diffuse.

From the dichromatic reflection model [19], the observed image color I is produced as the sum of a diffuse reflection component D and a specular component S:

$$I = D + S. \tag{1}$$

For a given iris pixel, there exist numerous possible combinations of diffuse and specular components that can produce its image color, so it is necessary to constrain the diffuse texture or specular illumination, or both, in the separation process. For the case of irises, both the texture and illumination can have complicated spatial variations, but the iris features described in the preceding section nevertheless provide information and constraints that allow our algorithm to determine an approximate separation. In the remainder of this section, we describe a technique for identifying diffuse colors and regions in an iris image, formulate the separation constraints from these diffuse colors and the characteristics of irises, and then combine these constraints within an energy function used to compute the separation.

3.1 Estimation of Iris Chromaticity

Our method begins by estimating the chromaticity of the iris, which facilitates the use of certain iris constraints. In computing this estimate, we make the assumption that some portion of the iris is unobscured by specular reflections. These unobscured iris areas often result from reflections of dark scene areas or from shadowing by eyelids. Although these iris regions may actually contain some very slight specular component, the specular magnitude is small enough in relation to the iris texture that we can approximate these regions as being diffuse. We also assume that the overall color spectrum of the illumination environment is approximately grey, a condition somewhat similar to the grey-world assumption in color constancy [10], so that diffuse iris regions have a chromaticity that lies on the iris chromaticity gamut described in Section 2.1, which was determined under white illumination. Some deviations from this condition, however, are seen in our results not to significantly impact the separation algorithm.

The chromaticity of an iris in a given image is determined by plotting the chromaticity values from the iris image and examining the points that lie along the iris chromaticity gamut line. While some of these points may result from specular reflections of light with a chromaticity similar to irises, most of these points cluster around the actual iris chromaticity. We note that light sources generally do not emit illumination the color of irises, since the locus of Planckian illuminant chromaticities [4] differs from that of the iris gamut. Furthermore, as exemplified in our experimental results, many typical illumination environments exhibit intensity variances in which relatively dark areas yield a fair number of diffuse iris pixels.

To identify the iris chromaticity value, we first sample points along the iris gamut and tabulate the number of pixels that project within a small radius of each sam-

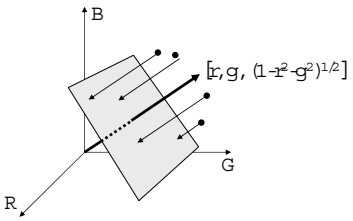

Figure 2. Mapping of colors in texture-independent image. Image color values are projected onto a plane defined by the iris chromaticity (r,g) to reduce the influence of iris color and texture.

ple. The sample with the maximum frequency is taken as the iris chromaticity, and pixels with chromaticity values within the radius of the iris chromaticity value are labelled as diffuse areas that do not exhibit an appreciable specular component. While some irises exhibit a variation of pigment concentration that results in multiple chromaticities, we present our method in regard to the case of irises without this variation, and then later describe how chromaticity variations affect our algorithm.

3.2 Illumination Correspondence

Irises typically appear in pairs, and a specular reflection over one iris often occurs over the other iris as well. For corresponding points of reflected illumination on the two irises, we form a constraint that their specular components should be the same.

When computing illumination correspondences between pixels of the two irises, the influence of iris texture needs to be reduced as much as possible. This can be done by projecting image colors onto a color-space plane defined by the iris chromaticity, as illustrated in Fig. 2. By suppressing color components along the iris chromaticity direction, we obtain a relatively *texture-independent image* suitable for illumination correspondence. The texture-independent image, we note, is not equivalent to the specular component, which may include some color along the direction of the iris chromaticity, but it nevertheless provides useful information on the illumination environment. Our correspondence method computes Hessian features in the texture-independent image, and then performs matching of these features in the iris pair along epipolar lines determined from the iris geometry [14].

Hessian features and correspondences of high confidence tend to be rather sparse because projecting 3D color into a 2D color plane reduces image variation and can increase the influence of noise, which masks subtle reflection features. Also, some corresponding specular reflections may differ in magnitude due to Fresnel reflectance effects, particularly for light from nearby objects that reflect off the two corneas from different incidence angles. In such cases, the correspondences will not be detected. However, in contrast to stereo, a dense correspondence is not necessary for our method. Our technique utilizes whatever confident correspondences are available, and for pixels without illumination correspondences, this constraint is not used.

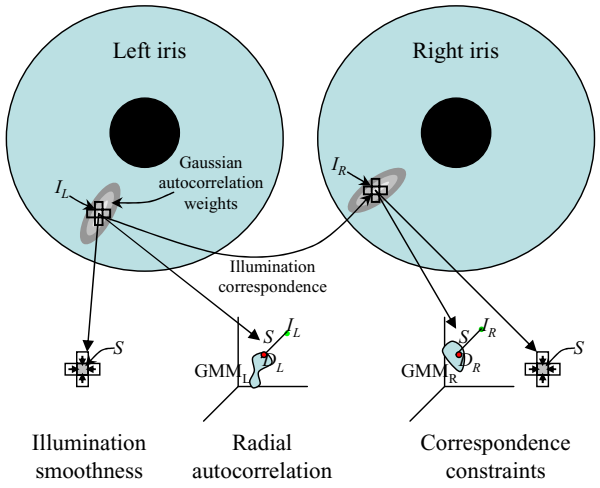

Figure 3. Constraints on specular component S. For a pixel in the left iris with image color I_L, the solution for its specular component S is constrained by the specular components of neighboring pixels (illumination smoothness), the diffuse components of radial neighbors (radial autocorrelation), and the parallel constraints for the pixel in the right iris with the corresponding illumination.

3.3 Illumination Smoothness

The texture-independent image not only provides information for illumination correspondence, but its edges indicate discontinuities in the illumination environment. In solving for the separation, we regularize the specular component so that it varies smoothly over the iris, but at each pixel this smoothness constraint is relaxed in proportion to the strength of its edges in the texture-independent image T. An energy measure for illumination smoothness is then formulated for pixel p as

$$L(S_p, p) = \sum_{q \in \boldsymbol{N_p}} ||S_q - S_p||^2 \, [1 - ||T_q - T_p||]^2$$

where S_p denotes the specular component at p, $\boldsymbol{N_p}$ is the set of 4-neighbors of p, and the RGB values of T are normalized to the range $[0, 1]$.

3.4 Radial Autocorrelation

Because of radial autocorrelation of iris textures, the diffuse component of an iris pixel is related to the diffuse components of neighboring pixels along the radial direction. To take advantange of this iris feature, our method forms for each pixel a probability model of its diffuse component based on the diffuse values in its neighborhood.

To emphasize the diffuse components of pixels lying closer to and in a radial direction from a given pixel, we weight the neighboring pixels according to a bivariate Gaussian function centered on the given pixel and oriented in the radial direction, as illustrated in Fig. 3. In our implementation, the standard deviation in the radial direction is set to 8% of the iris diameter, and in the perpendicular direction it is fixed to 3%. Pixels outside the iris or whose Gaussian values fall below a threshold are excluded from the neighborhood.

The weighted diffuse components form a distribution of texture colors in RGB space. We represent this color distribution using a Gaussian mixture model (GMM) of two univariate Gaussians computed by the EM algorithm. Then for a pixel p, the energy of a specular component S_p is expressed in terms of this texture GMM as

$$A(S_p, p) = \sum_{i=1}^{2} \alpha_i \mathcal{N}(p, I_p - S_p; \mu_i, \sigma_i)$$

where I_p is the image color of p, $I_p - S_p$ is the diffuse color of p, and $\alpha_i, \mu_i, \sigma_i$ are the magnitude, mean and standard deviation of Gaussian i.

3.5 Energy Function

The set of separation constraints can be expressed in terms of the specular illumination component S of a pixel, as illustrated in Fig. 3. The solution of S is dependent on smoothness of the specular component with respect to illumination discontinuities, texture autocorrelation along the radial direction, and the constraints associated with the pixel having a corresponding specular reflection, if a correspondence has been identified. It can be seen that these various constraints form a network both spatially with respect to illumination and texture, and between the two irises. In this way, various cues from different parts of the image are utilized together in solving for S.

To compute a separation result for irises, these constraints are combined into an energy function to be minimized. For pixels within the pupils, their diffuse texture is known to be black, so they are processed in a different manner. Because of dark current in CCD arrays, the diffuse component in pupils will have a nonzero value. This diffuse color is determined by simply fitting a five-Gaussian GMM to the pupil image colors, and then taking the color of the Gaussian center with the lowest intensity as the pupil diffuse color. The specular component on the pupil is calculated by subtracting this diffuse color from the image colors, with a minimum specular value of $(0, 0, 0)$.

Within the iris, for a pixel p without a corresponding pixel in the other iris, the energy of a specular value S_p can be expressed as

$$E(S_p, p) = L(S_p, p) + \beta A(S_p, p)$$

where β is an empirical constant. If an illumination correspondence p' is identified in the other iris, the energy of a common specular component S_p for both pixels can be written as

$$E(S_p, p) + E(S_p, p')$$

$$= L(S_p, p) + \beta A(S_p, p) + L(S_p, p') + \beta A(S_p, p')$$

To compute the separation over all the pixels in the two irises, the following total energy is minimized:

$$E(\boldsymbol{S}, \boldsymbol{S'}) = \sum_{p \in \boldsymbol{I}} E(S_p, p) + \sum_{p' \in \boldsymbol{I'}} E(S_{p'}, p') \qquad (2)$$

$$\text{such that } S_p = S_{p'} \text{ when } corr(p) = p'.$$

$\boldsymbol{I}$, $\boldsymbol{S}$, $\boldsymbol{I'}$, $\boldsymbol{S'}$ are the image colors and specular components of the left and right irises respectively, and $corr(p)$ represents the illumination correspondence of p if one is found. The first sum represents the energy for the left iris, and the second sum is for the right iris. Corresponding points between the two irises are constrained to have the same specular component.

The energy function in Eq. (2) is minimized by iteratively computing local solutions per pixel. The pixels are recursively processed in breadth-first order from the diffuse areas identified in Section 3.1. In the first iteration, pixels are processed in the left iris with texture GMMs constructed only using diffuse pixels and pixels whose diffuse component was computed earlier in the iteration. Correspondences are ignored in this first step, because diffuse and specular values have not yet been computed in the right iris. The next iteration similarly processes each pixel in the right iris, together with its corresponding pixel on the left. Subsequent iterations alternate between the two irises. For each pixel, a minimum energy is computed by the Levenberg-Marquardt method using three different initial values for the specular component S, based on the two Gaussian means of the texture GMM and the average specular value among its 4-neighbors.

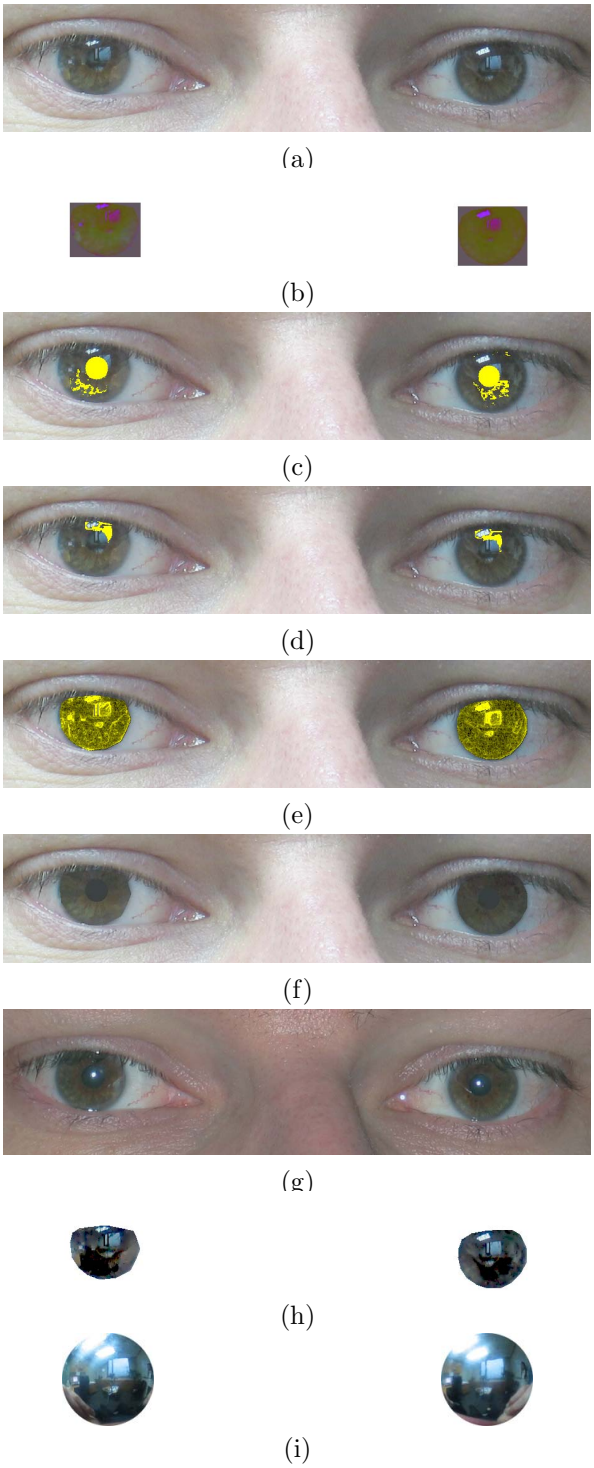

Figure 4. Results for green/hazel eyes. Images are gamma enhanced to increase clarity. For greater visual detail, please zoom in on the pdf version. (a) Original image, (b) Texture-independent iris colors, (c) Pupil and detected diffuse areas, (d) Illumination correspondence points, (e) Illumination edge strength (shown in degrees of yellow), (f) Our diffuse component, (g) Flash image which shows the iris texture, (h) Our specular component, (i) Illumination environment reflected from metallic spheres.

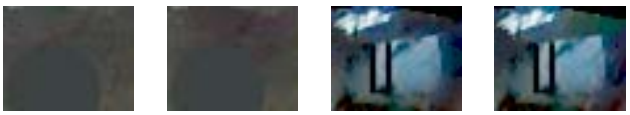

Figure 5. Close-up of illumination correspondence area in left eye of Fig. 4(d). Computed diffuse component: (a) with correspondence, (b) without correspondence. Computed specular component: (c) with correspondence, (d) without correspondence.

4 Results

Experiments with the proposed separation algorithm were performed on eyes of various colors in different environments. In converting a computed specular component into an illumination distribution, Fresnel reflectance should be accounted for with respect to the incident illumination angle at the cornea. Since the illumination directions of specular reflections can directly be computed from the mirror reflection law and the cornea geometry, which is fairly constant among people as previously mentioned, we present results for only the separation algorithm.

Fig. 4 displays a comprehensive set of results for an instance of green eyes shown in (a). The texture-independent image is shown in (b). Although some illumination detail is lost from this color transformation, the influence of iris texture on the resulting colors becomes negligible. The pupil and the identified diffuse areas are highlighted in (c), and the correspondence points in (d). The correspondences in this example are relatively few and concentrated in one area, but nonetheless contribute to the separation solution. Normalized illumination edge magnitudes for regulating illumination smoothness are shown in (e), and our estimated diffuse component is exhibited in (f). For comparison, an image taken with a bright flash is shown in (g) to give an idea of the iris texture pattern. Since the magnitude of the flash is substantially greater than the environment lighting, the environment reflections are mostly washed out by the bright diffuse texture, except for reflections of the nose. Our estimated specular component is displayed in (h), and an approximate illumination environment was captured by placing metal spheres in front of the eyes, as shown in (i). Since these spheres are not located precisely at the positions of the eyes, the recorded illumination environments are rather inexact; for example, they do not show reflections of the nose and eyelashes, or shadowing from the eyelids, and the subject's hands can be seen holding the spheres. Additionally, the field of view is not the same, but this image however provides a general idea of the surrounding scene.

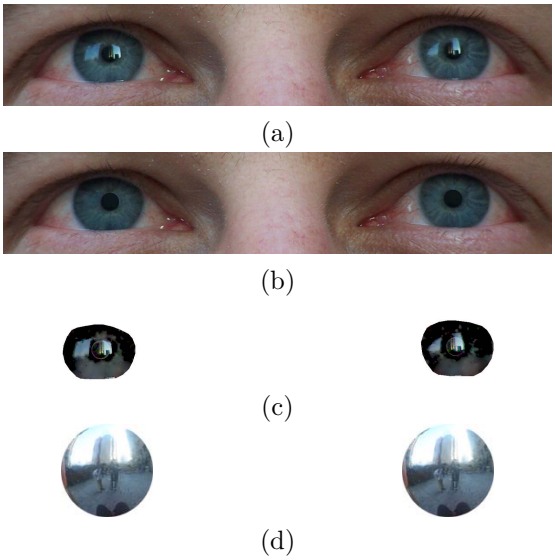

Figure 6. Results for blue eyes in an outdoor environment. (a) Original image, (b) Our diffuse component, (c) Our specular component (with gamma enhancement), (d) Illumination environment reflected from metallic spheres.

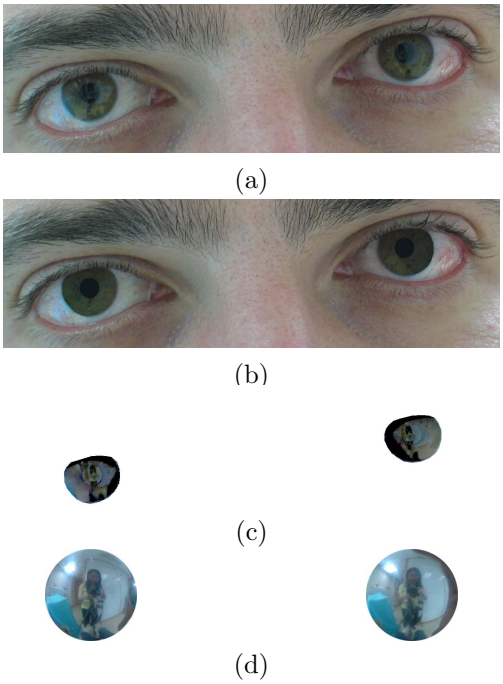

Figure 7. Results for green eyes in an indoor scene. (a) Original image, (b) Our diffuse component, (c) Our specular component (with gamma enhancement), (d) Illumination environment reflected from metallic spheres.

The effect of illumination correspondences is demonstrated in Fig. 5, which displays a close-up of a correspondence area given in Fig. 4(d). This region of the iris is relatively challenging because of the large number of surrounding high-magnitude edge points. Without the use of correspondences, separation accuracy is reduced as evidenced by some transfer of green iris color from the diffuse component to the specular component.

Given the difficulty of separating complex reflections from intricate texture, the illumination estimate is reasonable in that the majority of the more prominent reflections have been extracted. We note that because the iris colors are of similar magnitude to the environment reflections, the illumination environment cannot accurately be determined without performing separation. Although these principal reflections provide only a rough illumination estimate, it is nevertheless considerably more detailed than what can otherwise be obtained in a general image.

Noticeable in this example is some variation in eye color, where the area surrounding the pupil is hazel. In such regions where the iris color differs from the primary chromaticity computed in Section 3.1, a couple of problems may arise. One is that the iris texture in these regions may influence the texture-independent image. This may produce illumination edges that do not exist, which results in less reliance on the illumination smoothness constraint in these areas. The addition of this texture to the texture-independent image generally should not lead to many false illumination correspondences, because textures between a pair of eyes are independent of each other [1]. Reduced texture autocorrelation exists at transitions between different iris chromaticities, but this problem is mitigated somewhat when transitions are gradual. While our method is designed for the case of single chromaticity irises, some amount of chromaticity variation can be tolerated without significant degradation of separation results, as demonstrated in this example.

Fig. 6 exhibits a second example with blue eyes in an outdoor environment. Specular reflections of the sky can be seen on the similarly colored iris. Such instances are challenging for color-based separation methods, because the color difference between the specular and diffuse areas is close to a difference in shading. With the radial autocorrelation constraint for diffuse iris textures, this specular component can be separated. The grey street area is also extracted despite its subtle appearance in the eyes. Since the illumination from the sky is of much greater magnitude than that from the rest of the environment, many other reflections become too diminished for extraction.

In Fig. 7, we show a third example with green eyes in an indoor environment. Although the illumination estimate is somewhat rough, most of the major components of the illumination environment are separated.

5 Discussion

While much illumination reflects specularly from eyes, a substantial amount of light is also transmitted through the cornea. Consequently, the reflectivity of an eye is much lower than that of a mirrored sphere, and much light from an environment produces only dim reflections that may not be distinguishable from image noise. In scenes with strong sources of illumination, the diffuse component of an iris becomes bright, and this furthermore diminishes the visibility of weak specular reflections from the eyes. Nevertheless, the more prominent sources of scene illumination are often discernible, and contribute appreciably to the appearance of objects.

Certain illumination conditions can be problematic for our technique. In iris areas with visible, high frequency reflections full of illumination edges, the illumination smoothness constraint will be mostly inapplicable. If few illumination correspondences exist in these areas, then separation can only be computed from texture autocorrelation, which may lead to insufficient accuracy. Another troublesome illumination condition is bright lights that saturate image pixels. Since saturated pixels do not convey their actual scene colors, the dichromatic reflection model in Eq. (1) cannot be utilized, and consequently their specular components cannot be reliably estimated. The lack of information in saturated color values is a common problem in color-based computer vision methods.

Separation of corneal reflections in iris images is a difficult problem because of the complexity of both the illumination and iris texture. The separation obtained by our method is rather approximate and has a resolution limited by the iris image size, but it nevertheless provides an illumination estimate that is far more detailed than otherwise obtainable from an image that does not contain a special calibration object. Particularly for scene entities that are primarily diffuse such as human faces, this estimate of principal light contributions from the scene provides meaningful information for analyzing their appearance.

References

[1] J. Daugman. Iris recognition. *American Scientist*, 89:326–333, 2001.

[2] P. Debevec. Rendering synthetic objects into real scenes: Bridging traditional and image-based graphics with global illumination and high dynamic range photography. In *Proc. SIGGRAPH*, pages 189–198, 1998.

[3] S. Fan, C. R. Dyer, and L. Hubbard. Quantification and correction of iris color. Technical Report 1495, University of Wisconsin-Madison, Dec. 2003.

[4] G. D. Finlayson, S. D. Hordley, and M. S. Drew. Removing shadows from images. In *Proc. ECCV, LNCS 2353*, pages 823–836, 2002.

[5] J. V. Forrester, A. D. Dick, P. G. McMenamin, and W. R. Lee. *The eye: basic sciences in practice*. W B Saunders, Sydney, 2002.

[6] D. W. Hansen and A. Pece. Eye typing off the shelf. In *Proc. CVPR*, pages 159–164, 2004.

[7] D. R. Hougen and N. Ahuja. Estimation of the light source distribution and its use in integrated shape recovery from stereo and shading. In *Proc. ICCV*, pages 148–155, 1993.

[8] P. D. Imesch, I. H. L. Wallow, and D. M. Albert. The color of the human eye: A review of morphologic correlates and of some conditions that affect iridial pigmentation. *Survey of Ophthal.*, 41:117–123, Feb. 1997.

[9] G. J. Klinker, S. A. Shafer, and T. Kanade. The measurement of highlights in color images. *Int. J. of Computer Vision*, 2:7–32, 1990.

[10] E. H. Land. Recent advances in retinex theory. *Vision Research*, 26:7–21, 1986.

[11] A. Levin, A. Zomet, and Y. Weiss. Separating reflections from a single image using local features. In *Proc. CVPR*, pages 306–313, 2004.

[12] Y. Moses, Y. Adini, and S. Ullman. Face recognition: The problem of compensating for changes in illumination direction. In *Proc. ECCV*, pages 286–296, 1994.

[13] K. Nishino and S. Nayar. Eyes for relighting. *ACM Trans. on Graphics*, 23:704–711, 2004.

[14] K. Nishino and S. Nayar. The world in an eye. In *Proc. CVPR*, pages 444–451, 2004.

[15] S. J. Preece and E. Claridge. Monte carlo modelling of the spectral reflectance of the human eye. *Physics in Medicine and Biology*, 47:2863–2877, July 2002.

[16] I. Sato, Y. Sato, and K. Ikeuchi. Illumination distribution from brightness in shadows: Adaptive estimation of illumination distribution with unknown reflectance properties in shadow regions. In *Proc. ICCV*, pages 875–883, 1999.

[17] I. Sato, Y. Sato, and K. Ikeuchi. Illumination distribution from shadows. In *Proc. CVPR*, pages 306–312, 1999.

[18] I. Sato, Y. Sato, and K. Ikeuchi. Stability issues in recovering illumination distribution from brightness in shadows. In *Proc. CVPR*, pages II:400–407, 2001.

[19] S. Shafer. Using color to separate reflection components. *Color Res. and Appl.*, 10:210–218, 1985.

[20] P. Tan, S. Lin, L. Quan, and H.-Y. Shum. Highlight removal by illumination-constrained inpainting. In *Proc. ICCV*, pages 164–169, 2003.

[21] R. T. Tan and K. Ikeuchi. Separating reflection components of textured surfaces using a single image. In *Proc. ICCV*, pages 870–877, 2003.

[22] Y. Wang and D. Samaras. Estimation of multiple illuminants from a single image of arbitrary known geometry. In *Proc. ECCV, LNCS 2352*, pages 272–288, 2002.

[23] Y. Zhang and Y.-H. Yang. Multiple illuminant direction detection with application to image synthesis. *IEEE Trans. PAMI*, 23:915–920, 2001.

[24] Q. Zheng and R. Chellappa. Estimation of illuminant direction, albedo, and shape from shading. *IEEE Trans. PAMI*, 13:680–702, 1991.